

Sparsity-constrained Image Reconstruction in Optical Interferometry

D.L. Mary, B. Valat, O.J. Michel, F.-X. Schmider, B. Lopez

1 Abstract

In optical interferometry, the data available to reconstruct images are a few noisy points of their Fourier spectra. The image reconstruction problem is thus highly underdetermined. However, astronomical images are known to be highly compressible, meaning that they admit a sparse representation in some basis. This problem can be recasted as a Compressed Sensing (CS) problem, for which a lot of theoretical results and reconstruction algorithms have been elaborated in the recent years. We have started to investigate how some of these algorithms exploiting the sparsity of images could help in this problem in the case of upcoming phase referencing systems.

2 Underdetermined systems and sparse representations

– Consider the underdetermined problem $\underline{y} = V\underline{x}$, where $\underline{y} : (M, 1)$ is the observation vector; $V : (M, N)$ is the "sensing matrix" (accounts for acquisition + sparsity); $\underline{x} : (N, 1)$ is the unknown vector parameter (a vectorized image)
 $N > M \rightarrow$ Infinity of solutions

– CS approach : takes advantage of the prior information that \underline{x} is compressible, i.e. there exists a basis $W(N, N)$ where the representation \underline{u} of \underline{x} is **sparse** : $\underline{x} = W\underline{u}$, with $\text{supp}(\underline{u}) = |\underline{u}|_0 = S \ll N$
 S : sparsity of \underline{u}

– In general, wavelet bases are good compressors ("sparsifiers") for astronomical images. In particular, images of "unresolved" stars are sparse in direct space ($W = I$)

\Rightarrow Solution of the system obtained through :

$$\underline{u}^* = \underset{\underline{u}}{\text{argmin}} |\underline{u}|_0 \text{ subject to } \bigvee_{\Phi} \underline{u} = \underline{y}.$$

– Two questions :

1/ Theoretical : For a known vector \underline{y} , is \underline{u}^* unique ?

\rightarrow Yes if $\text{rank}(\Phi) \geq 2S$

\rightarrow For sufficiently small S : $\underset{\underline{u}}{\text{argmin}} |\underline{u}|_0 \Leftrightarrow \underset{\underline{u}}{\text{argmin}} |\underline{u}|_1$

\rightarrow Gribonval (2007) : can obtain the unique solution via L_p minimisation, $0 \leq p \leq 1$ ($L_p = (\sum |u_i|^p)^{\frac{1}{p}}$). Moreover for fixed S , L_p minimisation with $p < 1$ needs fewer measurements than with $p = 1$.

2/ Practical algorithms : if unique solution exists, how to find it ?

$\rightarrow L_0$ minimization : N-P hard

$\rightarrow L_1$ minimisation affordable via linear programming

$\rightarrow L_p$, $0 < p < 1$: efficient but non convex (local minima)

\rightarrow Greedy algorithms... (OMP, BP and variants)

– An approximate L_p minimization algorithm : IRLS (Rao 1999, Chartrand 2007) :

- Look for $\underset{\underline{u}}{\text{argmin}} (\mathcal{L} = \sum_i |u_i|^p - \lambda^t (\Phi \underline{u} - \underline{y}))$
- Get the fixed point equation :

$$\underline{u} = \underset{\underline{u}}{\text{diag}} \left\{ \frac{1}{|u_1|^{p-2}} \dots \frac{1}{|u_N|^{p-2}} \right\} \Phi^H (\Phi \Pi(\underline{u}) \Phi^H)^{-1} \underline{y}$$

• Whence the iterative algorithm :

$$\underline{u}^{(k+1)} = \Pi(\underline{u}^{(k)}) \Phi^H (\Phi \Pi(\underline{u}^{(k)}) \Phi^H)^{-1} \underline{y}$$

– Empirical success if :

$\rightarrow \underline{u}^{(0)} :=$ minimum energy (L_2) solution

\rightarrow algorithm is regularized : $\Pi_{ii}^{(k)} = (u_i^2 + \epsilon^{(k)})^{p/2-1}$.

– Can introduce a variable stepsize $\alpha^{(k)}$ to speed up convergence :

$$\underline{u}^{(k+1)} = \underline{u}^{(k)} - \frac{\alpha^{(k)}}{p} \Pi(\underline{u}^{(k)}) \nabla \mathcal{L}^{(k)}$$

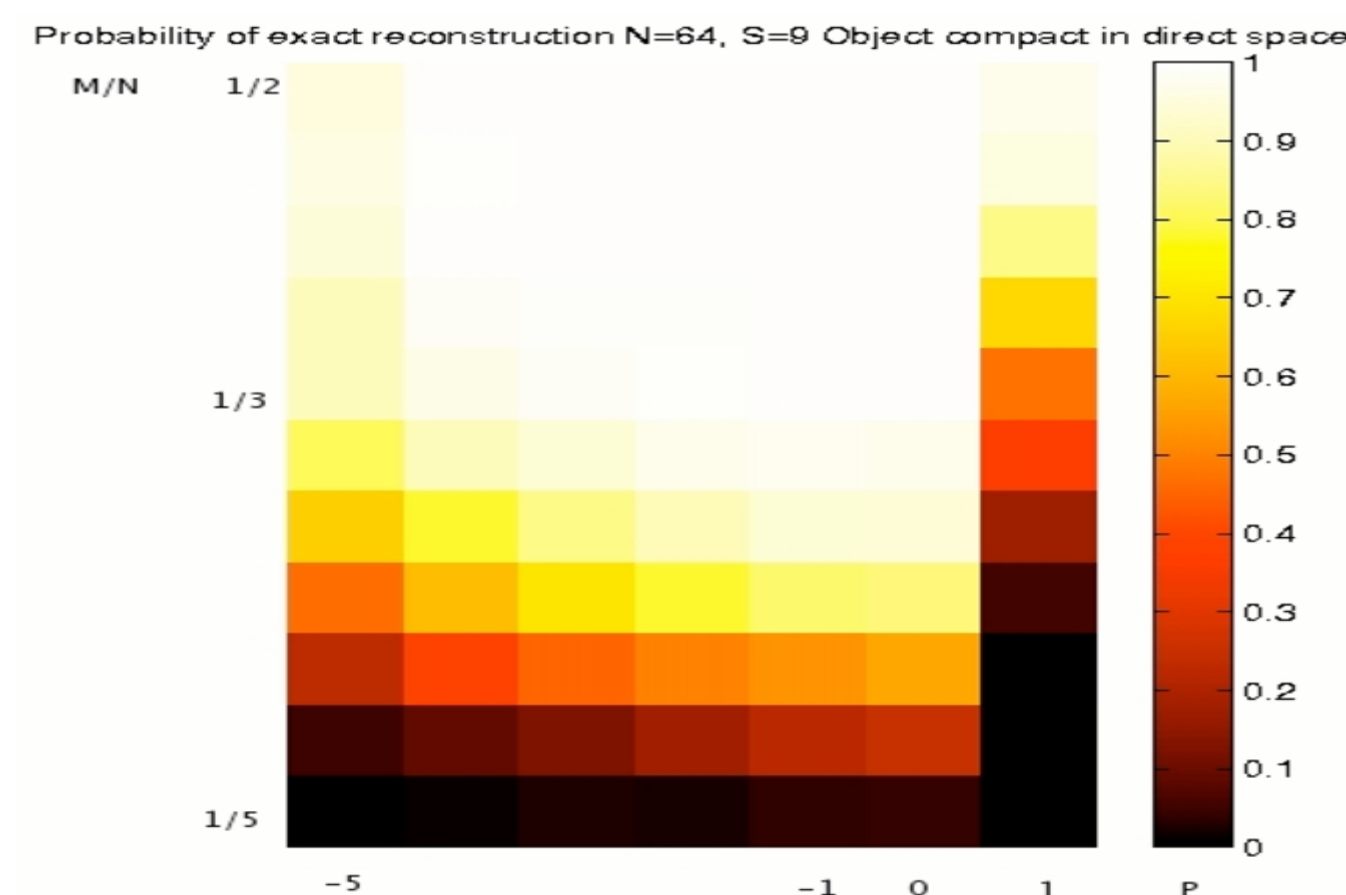


Fig. 1 : Comparison of exact reconstruction probability (white =1, black=0) for varying undetermination ratio $\frac{M}{N}$ and for various p (abscissa : $p = -5, -4, \dots, 0, 1$). The matrix Φ is a randomly undersampled 2D FT and the images are made of spikes (stars). Approximation of L_0 pseudo norm is the more efficient with this algorithm. Note that maximizing the L_p norm for $p < 0$ also leads to sparse representations.

3 Application to optical interferometry : noiseless case

In interferometry, interferences between the wavefront of the observed objects on two telescopes at position \underline{r}_i yields fringes. For an observation wavelength λ , the position of the fringes depends on the optical path difference of the two waves and on the phase of the object. The contrast of the fringes (the visibility) is the normalized Fourier Transform of the object at spatial frequency $\nu_i = \frac{\underline{r}_i}{\lambda}$.

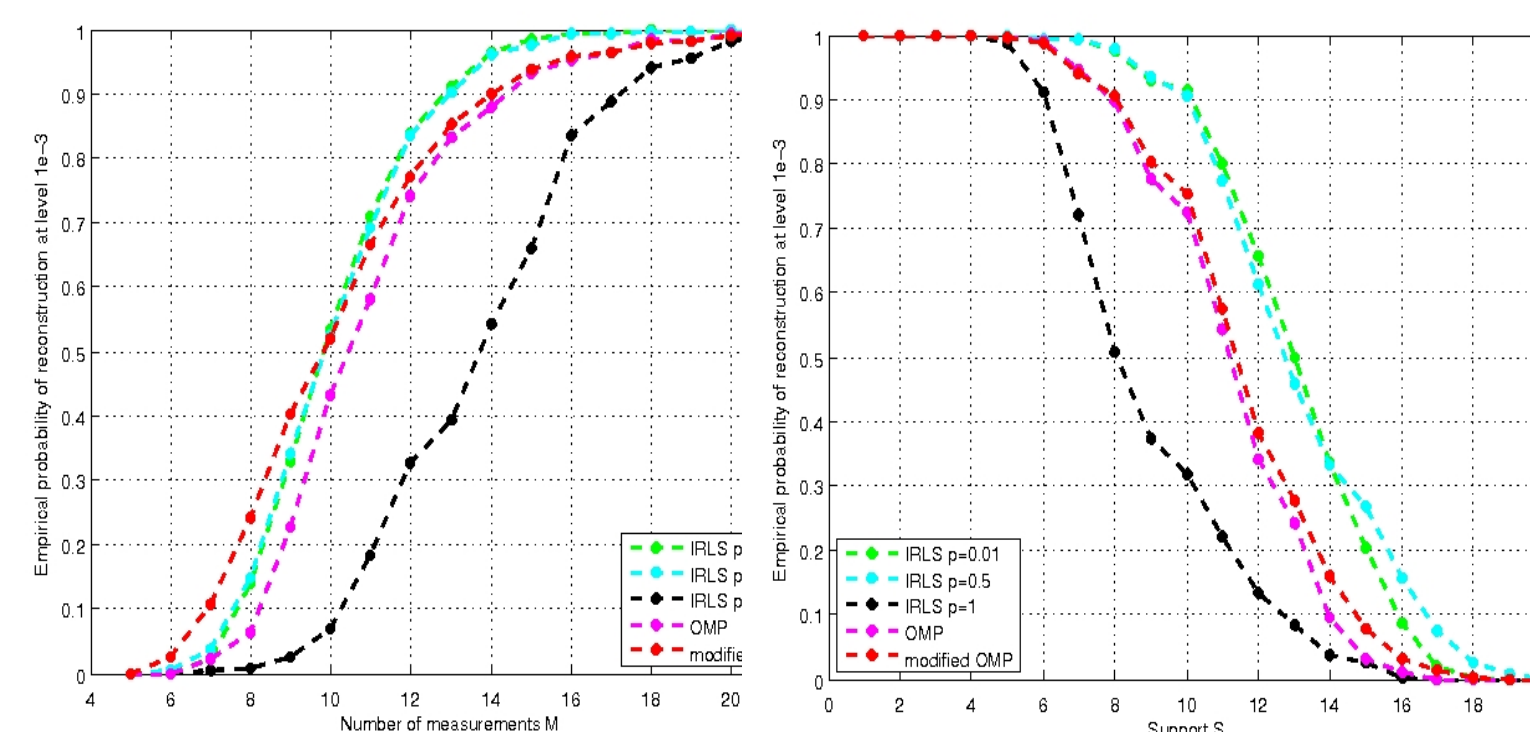


Fig. 2 : Comparison of the probability of reconstruction of IRLS (for $p=0, 0.5$ and 1) to two greedy algorithms. Greedy algorithms can behave relatively well w.r.t. more sophisticated optimization approaches while being computationally less complex. We also found that in presence of noise, OMP-like approaches are more robust to noise than IRLS.

4 Noise model in phase-referenced optical interferometry

– In current optical interferometric systems, the phases are known only through "phase closures". This case is not considered here.

– In the next few years however, we expect that (noisy) phases will be provided by the currently developed phase referencing systems. The phase reference will be obtained by observing simultaneously a reference star and a science object. It is possible to estimate the noise of such an observation on phase and visibility.

– The noise on the observed object phase can be estimated thanks to (see the Annex sheet for details) :

$$\sigma_{\phi}^2 = \frac{N_{*R} + N_{th} + M n_p \sigma_{read}^2 / 2}{(V_R(u) N_R(\lambda_i) / n_{tel})^2} + \frac{N_{*S} + N_{th} + M n_p \sigma_{read}^2 / 2}{(V_S(u) N_S(\lambda_i) / n_{tel})^2} + \dots$$

– The noise on the visibility can be estimated by :

$$\sigma_{Vis}^2 = \frac{N_{*} + N_{th} + M n_p \sigma_{read}^2}{\langle N \rangle^2} + \sigma_{jitter_on_vis}^2$$

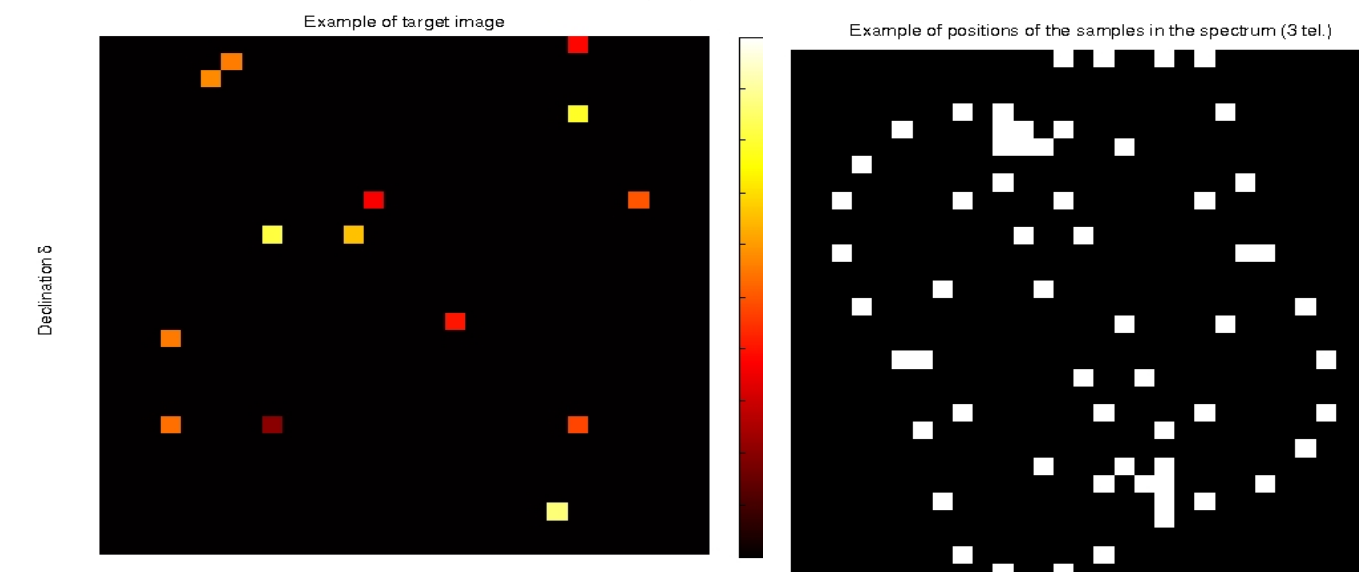


Fig. 3 : Simulation example using a configuration of 3 or 4 8m telescopes of VLT (configuration "A0 G1 K0 (G2)" at Paranal, Chili). Left : Original (simulated) star field with $S=20$ stars. Right : Example of location of 60 samples of the frequency spectrum obtained in one observing night.

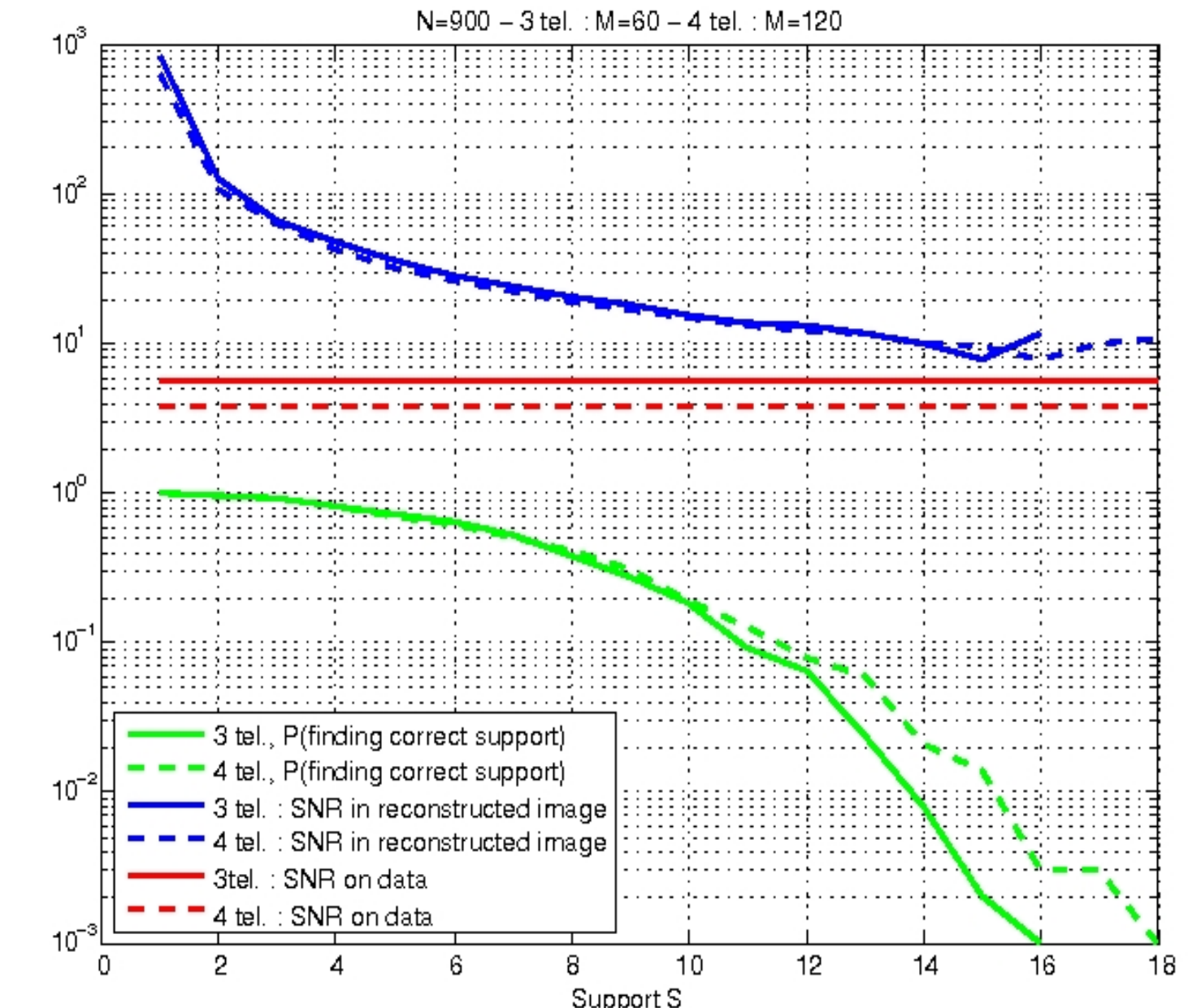


Fig. 4 : SNR in the data (red) and in the reconstructed images (blue) and reconstruction probabilities (green) using OMP for 3 (solid) and 4 (dashed) telescopes at Paranal. The red curves show that a typical SNR of 5 or so can be expected for a referencing system with the considered parameters. The blue curves show that at small S , the reconstruction algorithm (OMP) acts like a denoiser : the SNR is higher in the reconstruction images than in the instrumental data. (Inspection of the reconstructed images shows that at $\text{SNR} \approx 10$ original and reconstructed images can hardly be distinguished.) The green curves show that reconstructed images can be obtained with lower probability as S increases (and also indeed as the number of telescopes is less).

5 Conclusions

This preliminary study points out that for a given SNR in the data (≈ 5 to 10), images can in principle be reconstructed with a higher SNR (10 or more). The possibility of such a reconstruction is random but can be quantified (depends on Φ and on the support of \underline{u}).

Several important issues clearly need to be worked out, as :

- the robustness to noise of the reconstruction algorithm (e.g. IRLS with sparsity measure L_p , $p < 1$) ;
- the compromise sophistication vs complexity (Φ has no particular structure so it is difficult to avoid the natural scaling in $M \times N^2$ of the problem) ;
- finally the importance of an accurate instrumental model (noise + data acquisition) is crucial to set-up an efficient reconstruction method.

Indeed, another crucial point is that for different object types, different sparsity bases ($W \neq I$) need to be investigated as well.